DINAME 2023 - Proceedings of the XIX International Symposium on Dynamic Problems of Mechanics,
A.S. De Paula, A.T. Fabro and M.R. Machado (Editors), ABCM.
Pirenópolis, Go, Brazil, February 26th to March 3rd, 2023

Evaluation of Open Loop Onset Point Criterion to predict rate saturation PIO using flight simulator

Juliano A. B. Gripp [1], Marco A. G. Moreira [2], Luís G. Trabasso [3], and Cleverson M. P. Marinho [4]

[1,2,4] EMBRAER. Rod. Pres. Dutra, km 134, São José dos Campos, SP, 12247-820, Brazil

[3] ISI – Instituto SENAI de Inovação. R. Arno Waldemar Döhler, 308, Joinville, SC, 89218-153, Brazil

Abstract: Actuator rate saturation has been a contributing factor for Pilot-Induced Oscillations (PIO) experienced on some aircraft incidents, indicating potential design problems of flight control laws. Some criteria to predict this kind of phenomenon during design has been proposed in last decades, such as the Open Loop Onset Point (OLOP) criterion. In order to explore the capacities of prediction and limitations of OLOP criterion applied to the design of representative flight control laws for a transport aircraft in full flight envelope, two methods of control laws to regulate roll rate and sideslip ("p-beta") were evaluated, with different approaches for control allocation. OLOP criterion was applied in both methods with maneuvers varying pilot gain, frequency, and amplitude. These combinations were compared with pilot-in-the-loop simulations, using a flight simulator assisted by a robotic motion platform. It is possible to check that higher PIO ratings (worst cases) given by pilots are associated to cases with longer periods of rate-saturated actuator. However, OLOP criterion does not distinguish the duration of rate saturation, only its occurrence. Further recommendations to improve the process of clearance of control laws in the context of PIO due to rate limiting are proposed, adopting OLOP criterion as a first step.

Keywords: Nonlinear dynamics, Rate saturation, Open Loop Onset Point, Fly-by-wire, Robotic Flight Simulator

INTRODUCTION

Pilot-Induced Oscillation (PIO) problem has been present in aviation throughout the history of manned flight. PIOs have caused numerous accidents with results ranging from minor damage to total loss of the aircraft and pilot and it is still a challenging topic of recent works such as Efremov et al. (2020). The military standard MIL-STD-1797B (USAF, 2006) defines PIO as "sustained or uncontrollable oscillations resulting from efforts of the pilot to control the aircraft".

Some references such as GARTEUR (1999) present four categories to classify potentially severe PIOs: 1) Category I - Essentially Linear Pilot-Vehicle System Oscillations; 2) Category II - Quasi-Linear Pilot-Vehicle System Oscillations with Rate or Position Limiting (focus of this work); 3) Category III - Essentially Nonlinear Pilot-Vehicle System Oscillations with Transitions; 4) Category IV - Aeroservoelastic Coupling Oscillations.

The well-known theories for the analysis of Category I PIO focus on linear aircraft dynamics in the frequency domain, and the criteria documented for example in the following references are largely accepted: GARTEUR (1999), Neal and Smith (1971), Gibson (1990), Mitchell and Hoh (1999), Innocenti and Thukral (1991). However, the cited criteria are not enough to cover nonlinear effects in the frequency domain and predict Category II PIOs. Based on literature review, Open Loop Onset Point (OLOP) criterion from Duda (1997) is one of the most promising criteria to predict Category II PIOs, with a high degree of success for the cases evaluated, although some limitations have been found.

This paper highlights as contributions the evaluation of different control laws in flight simulator with pilot-in-the-loop in other to compare predictions of Category II PIOs given by OLOP criterion and pilot opinions. The target is to explore benefits and limitations of OLOP as a practical design tool. Next sections provide an overview of aircraft for case study, control laws, test matrix evaluated with pilots and overall results.

AIRCRAFT MODEL

To perform a representative flight control laws design, it is necessary to have detailed information about the aircraft. Considering the level of details from report such as NASA (1970), the airframe of the aircraft Boeing 747-100 (four-fanjet intercontinental transport aircraft) was adopted for this study. Figure 1(a) presents a schematic view of the aircraft, with emphasis in the control surfaces. This paper focuses attention on flap settings equal to 30 deg. Directional (yaw) control is obtained from two rudder segments (upper and lower rudder, assumed to move together). Lateral control system consists of inboard ailerons (High Speed Ailerons), outboard ailerons (Low Speed Ailerons) and roll spoilers. For simplicity, it is assumed that: inboard and outboard ailerons deflect together; only four most outboard spoiler panels (1, 2, 3, 4, 9, 10, 11, 12) were considered to actuate as roll spoilers. Moreover, it is assumed that the ailerons, rudders, and roll spoilers are driven by hydraulic actuators, with a full authority fly-by-wire control system.

A computational model for the aircraft (Figure 1(b)) was built using the software Simulink, described in Gripp et al. (2023a), and it was validated comparing simulation results with data from report NASA (1970). The model inputs are Throttle, deflection of Actuators and Mass Properties (Mass and Center of Gravity, CG). The main outputs are aircraft velocity (V), Pressure Altitude (Alt), angular rates (p, q, r), accelerations at CG (ax, ay, az), Euler angles (ϕ, θ, ψ) and aerodynamic angles (α, β, γ).

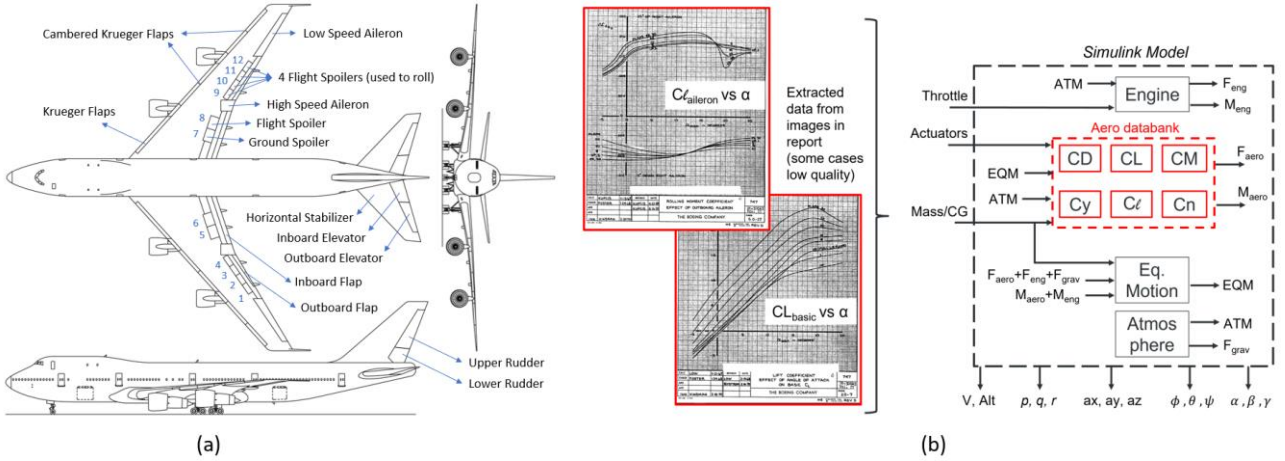

Figure 1 – (a) Views of Boeing 747-100. (b) Data extracted from report NASA (1970) to build aerodynamic model.

LATERAL-DIRECTIONAL CONTROL LAWS

In the context of aircraft lateral control (rolling axis), it is common to employ roll spoilers together with ailerons, working in collaborative way, in order to achieve requirements that ailerons only are not able to comply (low control power in some points of flight envelope for example). This is usually referred to as lateral control allocation. The challenge of control allocation in this context is to compute deflections of aileron and roll spoiler that comply with requirements of stability, performance, and handling qualities. Two approaches of control laws are proposed and adopted for case study in the context of PIO due to rate limiting (Category II). More details in Gripp et. al (2023b).

Method 1: Aileron + Roll spoiler with dead zone

One possible approach, called *Method 1* in this work, is to deflect only ailerons for small roll commands (cases of small corrections), but deflect ailerons together with spoilers in case of large roll commands (cases which require more agility). Moreover, in linear design, for sake of simplification, it is adopted a unique entity for lateral command (*Artificial Aileron*), which will be converted into actual deflections for aileron and roll spoilers during nonlinear design phase. This is a conservative approach to deal with nonlinear behavior of roll spoilers around small deflections for example, but can expose ailerons to rate saturation when deflecting alone in scenarios with poor control power.

Method 2: Aileron + Roll spoiler without dead zone

Another possible approach, called *Method 2* in this work, assumes the availability of a reliable aircraft model for design, specially capturing the nonlinearities of spoiler around neutral positions. With this approach, ailerons and roll spoilers deflect whenever there is lateral command. Roll spoiler can be tuned to provide initial moment with agility and reduce deflection in steady state. Following this approach, aileron and roll spoilers are designed separately. This approach alleviates the work of the ailerons, but it assumes a reliable model for design, which might be hard to develop.

Control objectives

This work adopted as case study two versions of regulators for ϕ' (Euler roll angle rate) and β (sideslip angle), using different methods of control allocation for aileron and roll spoilers. The selection of the regulated variables ϕ' and β is a natural one, since these are the variables that either a pilot or an autopilot shall control in order to achieve the desired trajectory path in terms of lateral-directional dynamics. The control architectures analyzed in this study are adaptations of usual controllers referred to in literature as “p-beta” (controllers for roll rate and angle of sideslip), such as presented in the references Berger et al. (2013), Gripp (2015). Related longitudinal control laws for same aircraft are described in the reference Moreira et al. (2022).

FLIGHT SIMULATIONS WITH PILOT-IN-THE-LOOP

Flight Simulator overview

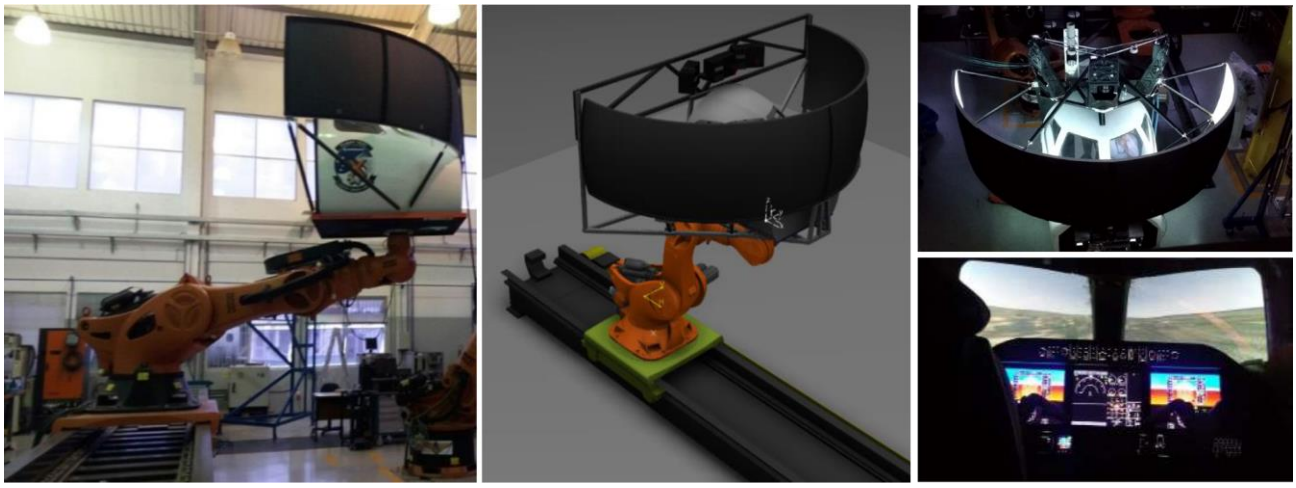

Figure 2 - External and internal views of SIVOR Flight Simulator, Silva et al. (2019).

For this work, a flight simulator assisted by a robotic motion platform (called "SIVOR", acronym for "*Simulador de Voo com Plataforma Robótica de Movimento*"), installed at ITA ("Instituto Tecnológico de Aeronáutica", Brazil) facilities was selected as platform for tests. SIVOR simulator is a motion-based flight simulator under development at ITA in partnership with Embraer company (Oliveira et al. (2019), Silva et al. (2019)). The SIVOR robot, a "KUKA KR-Titan", has a payload of 1,000 kg, making it possible to carry a high-fidelity cabin of a small aircraft, as illustrated in Figure 2. For sake of scope reduction, without compromising conclusions of this work, the tests with pilots were conducted like in a usual fixed-base flight simulator (i.e., motion disabled). Although the selected airframe corresponds to Boing 747-100, sidesticks were adapted as lateral inceptors for flight simulations, facilitating investigations of Category II PIO. Other important available inceptors for this test are rudder pedals, throttle levers, flap levers.

Handling Qualities task definition

In order to check the characteristics of aircraft and flight control laws in the context of Category II PIO, it is necessary to force the Pilot-Vehicle System to enter in possible PIO prone conditions due to rate limiting. The proposed methodology was to perform some tracking tasks with different profiles. A target symbol (flight director) was programmed to display on Primary Flight Display (PFD) a tracking reference for the pilot (Figure 3). In practical terms, the pilot task is to track as much and quick as possible the flight director in PFD (magenta symbol in Figure 3). Current flight path is represented by green symbol in Figure 3.

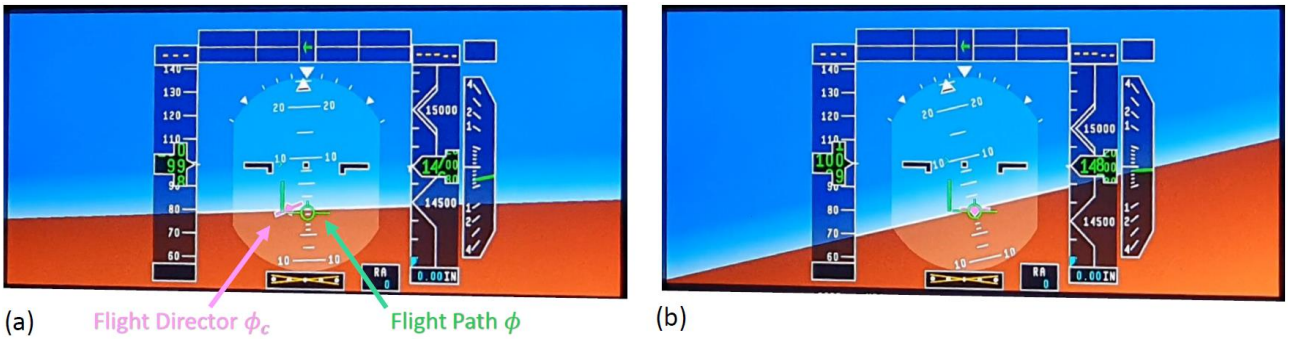

Figure 3 - Screenshots of PFD. (a) Pilot looking for tracking. (b) Target tracked.

Figure 4(a)/(b)/(c)/(d) illustrate four profiles along time for tracking reference (ϕ_c), for evaluation of handling qualities and identification of possible PIO tendencies. Figure 4(a) represents a sinusoidal waveform adopted to directly check the predictions of OLOP criterion in certain frequency (ω_{onset}, the frequency at which actuator saturation occurs for the first time). This sinusoidal waveform is composed by 5 sinusoidal cycles with frequency equal to 70% of the investigated ω_{onset} and 5 sinusoidal cycles with frequency equal to ω_{onset}, providing a gradual entrance into the predicted scenario of rate limiting. The amplitude of this sinusoidal waveform is changed in different trials in order to cover different possibilities of pilot gains and check rate limitation (there was no confidence about pilot gains in advance).

Discrete tracking task is based on the methodology presented by MIL-STD-1797B (USAF, 2006). According to references such as Mitchell and Klyde (2004), discrete tracking provides good exposure to Category II PIO, since it provides combination of fine-tracking and gross acquisition in a high-pilot-gain task. Figure 4(b) presents an example of

discrete tracking reference. The amplitude and shape of the discrete task was defined as a compromise between the capacity of the aircraft to follow the reference and enough changes to stimulate abrupt commands.

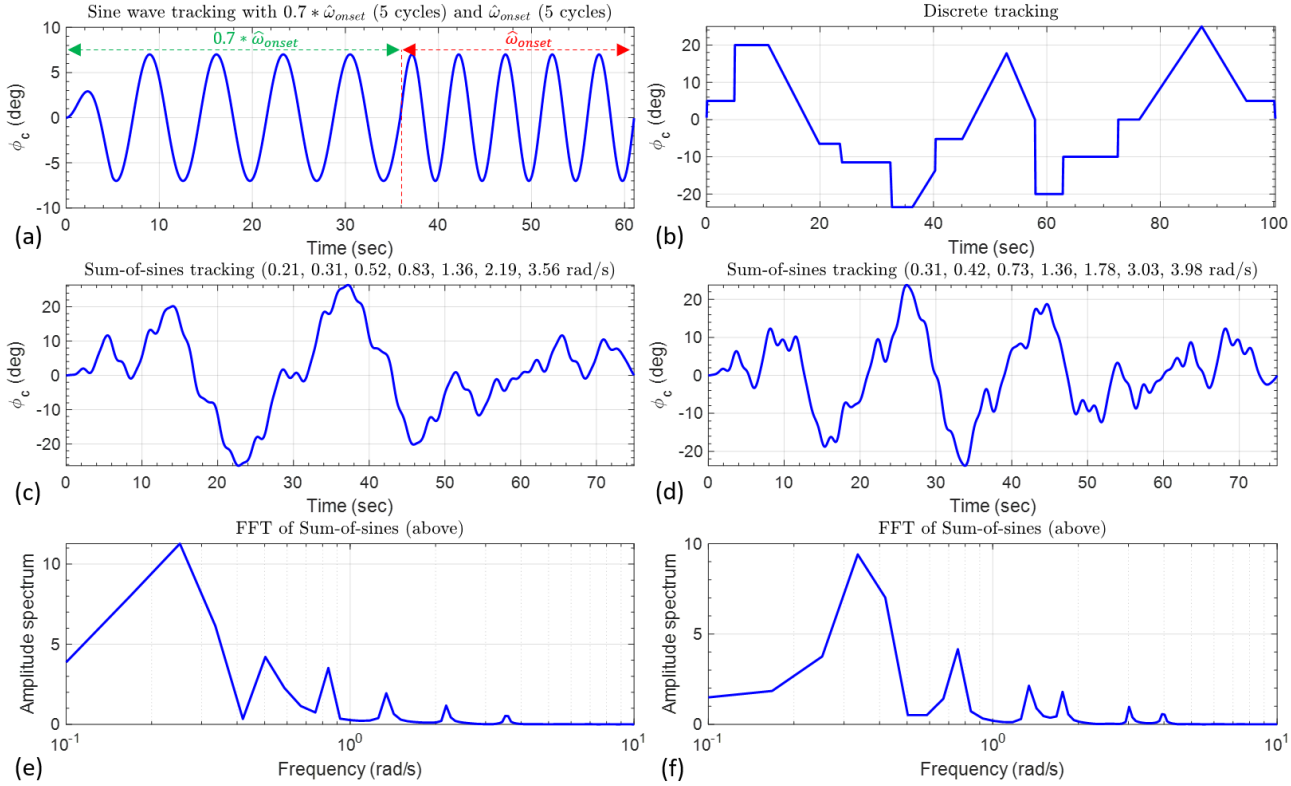

Figure 4 - Maneuvers for tracking reference (ϕ_c): (a) Sines waves; (b) Discrete tracking; (c)/(d) Sum-of sines; (e)/(f) FFT of (c)/(d) respectively.

Sum-of-sines tracking task is based on the methodology of the Air Force Handling Qualities Demonstration Maneuver Catalog (Klyde and Mitchell, (1997)). Figure 4(c)/(d) present examples of sum-of-sines tracking reference. This kind of maneuver allows to sweep a range of frequencies during the same maneuver, which provides data to identify the pilot frequency response for example (further analysis presented in section "Identification of pilot model"). Following guidelines from Klyde et at. (2015), the profiles presented in the Figure 4(c)/(d) have the characteristics summarized in the Table 1. The amplitudes of sum-of-sines were set to have root mean square (RMS) equal to 5.92 deg (Figure 4(c)) and 9.74 deg (Figure 4(d)), decreasing values along frequencies (power spectrum density decays as frequency increases). The frequencies of sum-of-sines were selected in order to have a balanced distribution in the range of interest (see Fast Fourier Transforms, FFT, Figure 4(e)/(f) with logarithm axis), whose definitions follow Fibonacci values in terms of number of cycles. Complete maneuvers have 75 seconds, in which the amplitude ramps in from zero to full amplitude over the first five seconds and the signal ramps out over five seconds at the end of the run.

Table 1 – Amplitudes (A_i) and frequencies (ω_i) for Sum-of-sines tracking tasks (Figure 4(c)/(d)).

	Figure 4(c)		Figure 4(d)	
i	ω_i [rad/s]	A_i (deg)	ω_i [rad/s]	A_i (deg)
1	0.21	7.00	0.31	11.00
2	0.31	-4.67	0.42	-8.25
3	0.52	2.80	0.73	4.71
4	0.84	-1.75	1.36	-2.54
5	1.36	1.08	1.78	1.94
6	2.20	-0.67	3.04	-1.14
7	3.56	0.41	3.98	0.87

Flight simulation configurations and results

A methodology for flight simulations with pilot-in-the-loop was defined based on literature references (such as Berger et al. (2021), Klyde et al. (2015)) as well as background experience of authors. In order to define a representative scope for comparison of offline predictions from OLOP criterion and classical PIO ratings from pilots, the following combinations were selected: 1) two flight conditions in the operational envelope of Flaps 30 deg with low speed (100 KCAS): Pressure Altitudes of 15,000ft and 3,000ft. The rationale behind was to select example of flight conditions with potential rate limitations in control surfaces due to low control power; 2) three types of tracking tasks,

as presented in Figure 4; 3) two versions of control laws (version of "p-beta": Method 1 and 2); 4) two flight test pilots (called "A" and "B") with large experience in handling qualities analysis in different classes of aircraft.

For each combination of flight simulation, some metrics were extracted from pilot opinion and time histories: 1) PIO ratings (PIOR), following PIO tendency classification (USAF, (2006)); 2) Phase delay, from pilot command (ϕ'_{cmd}) to aircraft actual roll rate (p); 3) Percentage of time that aileron remains saturated; 4) Percentage of time that roll angle (ϕ) remains out of boundaries defined by a tolerance of 5 deg during maneuver; 5) Occurrences of aileron saturation with duration larger than 0.5 sec.

Figure 5 illustrates some flight tests performed at SIVOR with pilot-in-the-loop to evaluate the "p-beta" control laws. Initial tests were performed to assure that the designed control laws are acceptable for the aircraft (Gripp et al. (2023b)), as well as check that the simulation environment (stick, pedals, throttles, visual, Primary Flight Display) is representative for handing qualities evaluation and PIO investigation. After validation of control laws and flight simulator by both pilots, specific maneuvers (depicted in Figure 4) were performed to investigate Category II PIO.

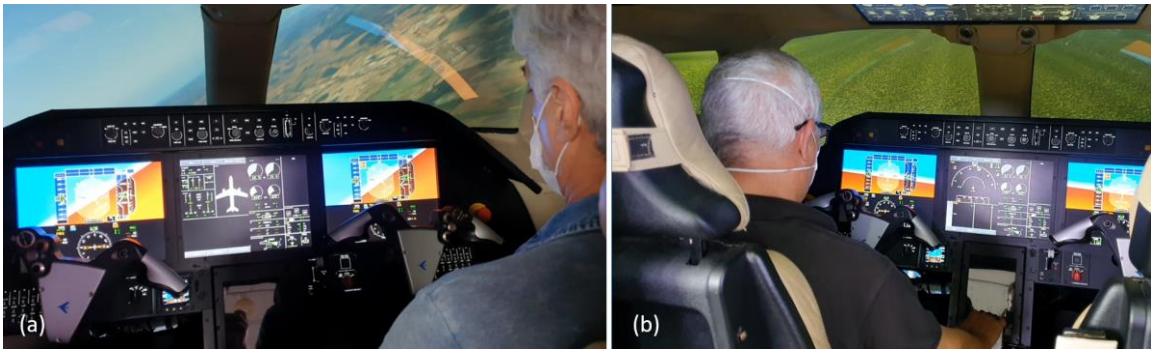

Figure 5 – Tests in SIVOR with pilot-in-the-loop.

Table 2 presents a summary of flight simulation campaign at SIVOR simulator (proposed test matrix and results).

Table 2 – Summary of flight simulations at SIVOR (Flaps=30 deg / 350,000 lb / CG=33% / 100 KCAS)

Configuration and task						Pilot A					Pilot B				
#	Alt [ft]	Task	p-beta Method	|ϕc| (deg)	ω_{onset} (rad/s)	PIOR	Phase Delay ϕ' to p (deg)	% of time Ail. Sat.	% of time out of tol.	Sat. with Δt>0.5sec	PIOR	Phase Delay ϕ' to p (deg)	% of time Ail. Sat.	% of time out of tol.	Sat. with Δt>0.5sec
1	15,000	Sine Fig. 4 (a)	1	7	1.25	2	165	18.8	N/A	5	2	88	32.1	N/A	5
2	15,000	Sine Fig. 4 (a)	2	7	1.25	2	82	1.3	N/A	0	1 to 2	75	2.2	N/A	0
3	15,000	Sine Fig. 4 (a)	1	9	1.25	2	158	22.7	N/A	4	2	113	28.8	N/A	2
4	15,000	Sine Fig. 4 (a)	2	9	1.25	2 to 3	108	6.3	N/A	4	2	97	2.3	N/A	2
5	15,000	Sine Fig. 4 (a)	1	11	1.25	3 to 4	176	17.4	N/A	10	3	116	20.4	N/A	3
6	15,000	Sine Fig. 4 (a)	2	11	1.25	3	124	9.4	N/A	4	2 to 3	102	3.5	N/A	2
7	15,000	Sum-of-Sines Fig. 4 (c)	1	N/A	N/A	2	N/A	31.7	38.9	5	2	N/A	27.7	47.1	5
8	15,000	Sum-of-Sines Fig. 4 (c)	2	N/A	N/A	2	N/A	0.1	39.2	0	2	N/A	0.2	49.1	0
9	15,000	Sum-of-Sines Fig. 4 (d)	1	N/A	N/A	3	N/A	35.3	46	11	2	N/A	30.5	44.7	11
10	15,000	Sum-of-Sines Fig. 4 (d)	2	N/A	N/A	2	N/A	1.1	44.5	0	2	N/A	1.4	48.3	0
11	15,000	Discrete Fig. 4 (b)	1	N/A	N/A	1	N/A	30.4	12.3	0	2	N/A	15.9	28.4	5
12	15,000	Discrete Fig. 4 (b)	2	N/A	N/A	1	N/A	0	15	0	1 to 2	N/A	1.4	19.8	0
13	3,000	Sine Fig. 4 (a)	1	5	1.35	1 to 2	92	19.2	N/A	0	1 to 2	53	41	N/A	0
14	3,000	Sine Fig. 4 (a)	2	5	1.35	2	68	0.2	N/A	0	1 to 2	55	0	N/A	0
15	3,000	Sine Fig. 4 (a)	1	7	1.35	2	149	21.2	N/A	0	2	82	31.7	N/A	0
16	3,000	Sine Fig. 4 (a)	2	7	1.35	2	70	0	N/A	0	1 to 2	66	0.1	N/A	0
17	3,000	Sine Fig. 4 (a)	1	10	1.35	3	155	20.4	N/A	4	3	144	31.7	N/A	5
18	3,000	Sine Fig. 4 (a)	2	10	1.35	2 to 3	134	5.7	N/A	4	3	113	2.7	N/A	0
19	3,000	Sum-of-Sines Fig. 4 (c)	1	N/A	N/A	2	N/A	18.8	47.4	1	2 to 3	N/A	27.2	55.3	3
20	3,000	Sum-of-Sines Fig. 4 (c)	2	N/A	N/A	2	N/A	0	41.5	0	2 to 3	N/A	1.3	48.2	1
21	3,000	Sum-of-Sines Fig. 4 (d)	1	N/A	N/A	2	N/A	29.9	38.9	2	2	N/A	35.5	54.6	9
22	3,000	Sum-of-Sines Fig. 4 (d)	2	N/A	N/A	2	N/A	0.2	41.3	0	2	N/A	2.3	49.7	0
23	3,000	Discrete Fig. 4 (b)	1	N/A	N/A	2	N/A	18.9	14.2	1	2	N/A	26.7	27	4
24	3,000	Discrete Fig. 4 (b)	2	N/A	N/A	1	N/A	0.1	13.1	0	1 to 2	N/A	0.6	20.1	0

To illustrate how data were extracted, Figure 6 presents some time histories for sinusoidal tracking. In this example, same tracking reference ($|\phi_c|$=5deg and ω_{onset} =1.35rad/s) was selected. Even though the same tracking reference was presented to both pilots, Pilot A applied lower amplitudes of command than Pilot B in these examples. The peaks of ϕ'_{cmd} for Pilot A usually are lower than 10 deg/s (75% of command authority), but peaks of ϕ'_{cmd} for Pilot B are greater, achieving 15 deg/s (100% of command authority) many times. It indicates that the pilots have slightly different gains.

For both pilots, the occurrences of rate saturation in ailerons for "p-Beta" with Method 1 (with roll spoiler dead zone) are much more common than "p-Beta" with Method 2. For "p-Beta" with Method 1, Aileron remained saturated 19.2% of time during maneuver for Pilot A and 41% of time for Pilot B. However, aileron remains saturated by short periods when it occurs, less than 0.5 seconds in this example (there are other maneuvers in which aileron remained saturated for longer periods). The period of saturation and its effects in handling are not covered by OLOP criterion, thus it is topic for improvement. In terms of roll spoiler saturation, there are some occurrences for both pilots and "p-Beta" Methods.

The computed phase delay is given by a mean delay in time between pilot command (ϕ'_{cmd}) and aircraft roll rate response (p), divided by period of oscillation ($1/\omega_{onset}$), and multiplied to 360 deg to convert to degrees. For the example presented, the phase delay of Pilot A was 92 deg for Method 1 and 68 deg for Method 2. It could indicate that Method 2 is slightly better than 1, which is compatible with time response, especially when ϕ'_{cmd} have peaks and p cannot follow. However, Pilot B obtained similar results in terms of phase delay for both Methods 1 and 2 (53 and 55 deg respectively).

Finally, the PIO ratings given by the pilots are similar (around 1 to 2) specifically in this example, which is not conclusive to determine if one version of control law is much better than other. It is necessary to compare other metrics and other configurations.

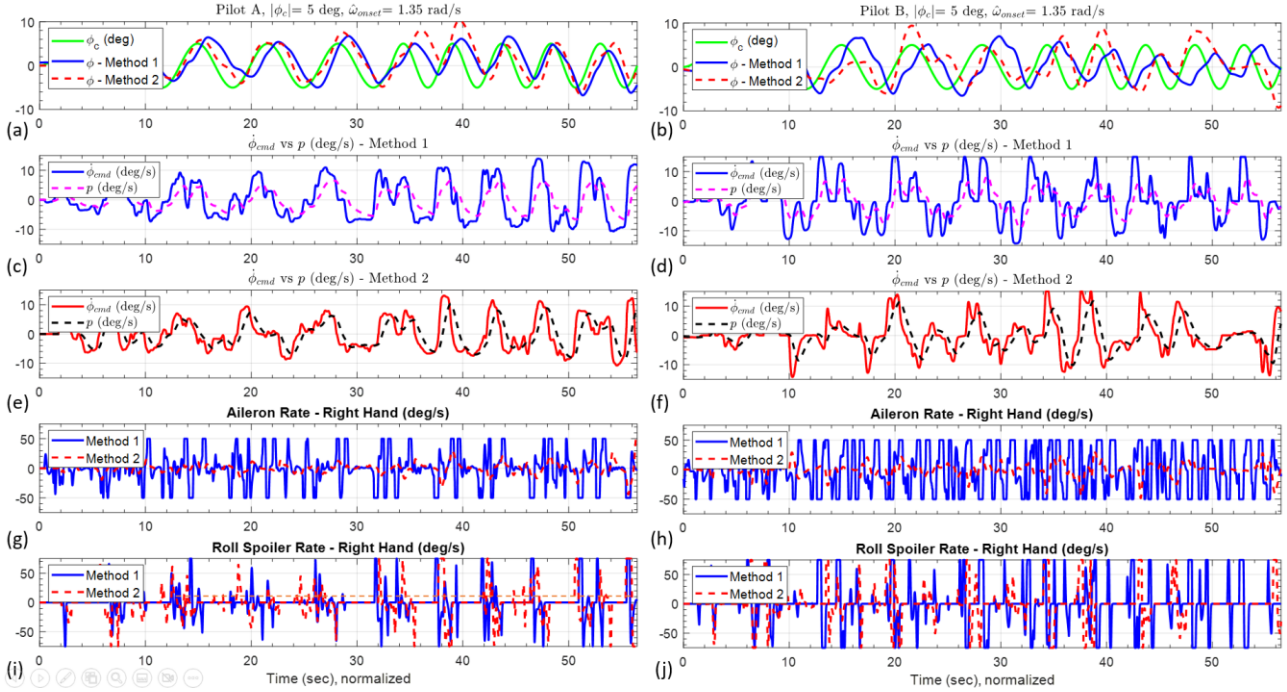

Figure 6 – Example of sinusoidal tracking with amplitude of ϕ_c equal to 5 deg and ω_{onset} =1.35 rad/s (points #13 and #14 from Table 2, for Pilot A (left) and Pilot B (right): (a)/(b) Reference ϕ_c vs actual ϕ. (c)/(d)/(e)/(f) Comparison of command ϕ'_{cmd} and roll rate response p. (g)/(h) Aileron rates. (i)/(j) Roll Spoiler rates.

Additionally, Figure 7 presents examples of results for sum-of-sines and discrete tracking, for Pilot B (points #21 to #24 from Table 2). The percentage of time that ϕ is out of tolerance boundaries ($\phi_c \pm$ 5 deg) is slightly better in Method 2 for both maneuvers: 54.6% versus 49.7% in sum-of-sines, 27% versus 20.1% in discrete task, comparing Method 1 and 2 respectively. However, this metric is not the driver to determine which control law is more PIO prone.

It is more evident the number of occurrences involving aileron rate saturation. In both maneuvers, Method 1 presents several occurrences of aileron saturation, and many of them for more than 0.5 seconds (9 cases in Sum-of-Sines and 4 cases in Discrete Task). It is an indicative that Method 1 is more exposed to Category II PIO, although the PIO ratings given by pilots do not present significant changes.

Finally, the results obtained with pilot-in-the-loop using flight simulator can be compared with offline results documented in Gripp et al. (2023c). The highlights are:

- the evaluations of pilots confirmed what was predicted by OLOP criterion: "p-Beta" with Method 1 (with spoiler dead zone) is more likely to develop Category II PIO if compared to Method 2 (no spoiler dead zone);
- it is possible to check that higher PIO ratings (worst cases) are associated to cases with longer periods of rate-saturated aileron (more than 0.5 sec);
- some cases with different predictions of Category II PIO according to OLOP criterion have similar PIO ratings given by pilots. It might be justified because rate saturation occurs as predicted by OLOP criterion, but by short periods. Therefore, the pilots did not distinguish significant differences;

- OLOP criterion gives guidelines to identify Category II PIO prone cases, but it does not cover the influence of the duration that the control surface remains saturated. It is a significant aggravating to be considered, it is not enough to check only peaks of saturation.

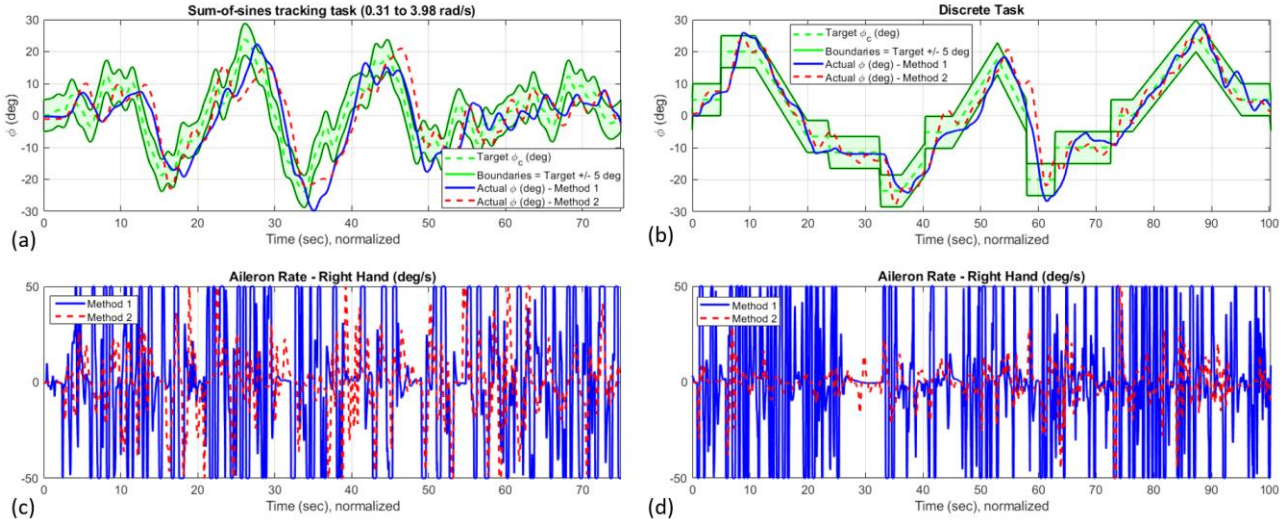

Figure 7 – Example of sum-of-sines and discrete tasks for Pilot B (points #21 to #24 from Table 3): (a)/(b) Reference ϕ_c vs actual ϕ. (c)/(d) Aileron rates.

Identification of pilot model

For some applications such as a compensatory tracking task with random input it is possible to model the pilot with a low order transfer function. In this context the operator uses only tracking error ($\phi_{error} = \phi_c - \phi$, in this work) to track an unpredictable target (ϕ_c) presented on the Primary Flight Display (PFD). A usual approach to model the pilot behavior (ϕ_{error} to ϕ'_{cmd} , in this work) is given by Equation 1, based on references such as Neal and Smith (1971), McRuer (1995):

$$\phi'_{cmd}(s)/\,\phi_{\text{error}}(s) = (\text{Kp}\,(T_{lead}.s + 1)\,e^{-\tau_p s})/(\,T_{\text{lag}}\;s + 1) \tag{1}$$

where the following parameters are empirically determined: Kp (pilot gain), T_{lead} (lead time constant), T_{lag} (lag time constant), τ_p (neuromuscular delay). The parameters Kp, T_{lead} , T_{lag} represent the capability of the pilot to optimize his control of a given task, i.e., the pilot may use lag compensation to achieve high gain and fine control in some low-bandwidth tasks, or lead compensation to achieve high bandwidths in others (Stevens and Lewis (1992)). Moreover, this kind of pilot model is not just a pure pilot gain (which is best fitted to full developed PIO) but rather a model that is better adjusted to the moment before PIO phenomenon starts.

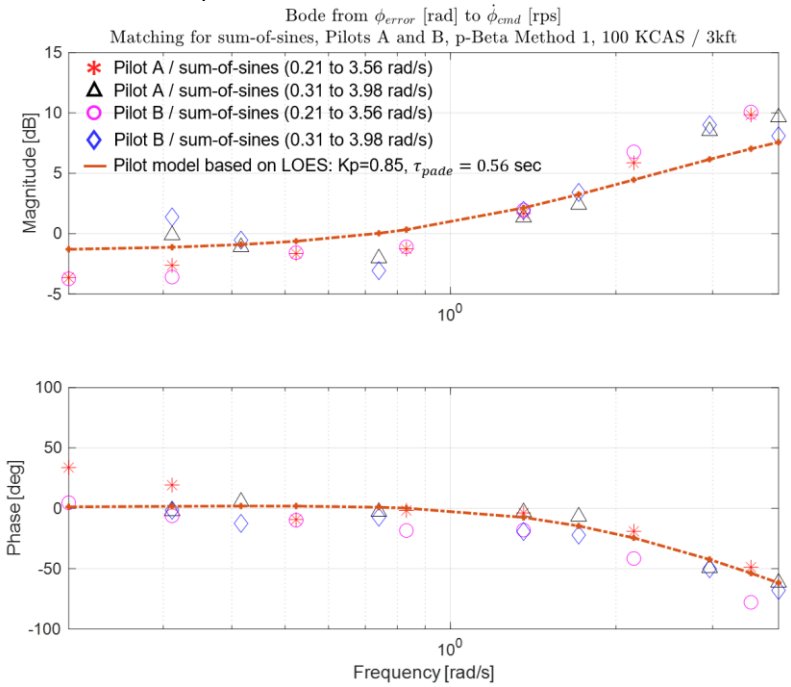

Figure 8 - Example of pilot model identification (points #19 to #22 of Table 2, Pilots A and B, "p-Beta" Method 1): frequency response ϕ_{error} to ϕ'_{cmd}, highlighting magnitudes and phases at frequencies for sum-of-sines.

An approach for data fitting, considering Equation 1, is to replace the term $e^{-\tau p.s}$ by a first order Padé approximation model. This is one approach to get a Lower Order Equivalent System (LOES), following references such as Mitchell and Hoh (1982), Morelli (2000), USAF (2006). For this example, consider a cost function J as follows:

$$J = \sum_{i=1...n} (Mag_{ref} - Mag_{model})^2 + (Phase_{ref} - Phase_{model})^2 \quad (2)$$

where n = 12 is the number of frequencies under analysis in this example (union from sum-of-sines, Table 1), Mag_{ref} and $Phase_{ref}$ are the magnitude and phase reference data from pilots (see Figure 8), Mag_{model} and $Phase_{model}$ are the magnitude and phase from model subject to identification (LOES). In order to obtain a Lower Order Equivalent System (LOES), an optimization process was conducted to minimize the cost function J from Equation 2. The variables of optimization are Kp, T_{lead} , T_{lag}, and the Padé approximation time delay, named τ_{pade}. The result of this optimization process is presented in Equation 3 and plotted in Figure 8 (dash-dot orange). This approach illustrates how to obtain a pilot model to evaluate OLOP criterion, closer to actual data, instead of adopting extreme pure pilot gains as proposed by Duda (1997). Similar process can be repeated for other cases from Table 2 to estimate representative pilot models.

$$\phi'_{cmd}(s) / \phi_{\text{error}}(s) = ((0.85\ (0.88\ s + 1)) / (0.21\ s + 1))\ (\text{-s+3.535}) / (\text{s+3.535}) \quad (3)$$

PROPOSAL OF PROCESS FOR CLEARANCE OF FLIGHT CONTROL LAWS CONSIDERING CATEGORY II PIO

Based on results presented in previous sections and accumulated background of authors in industrial experience, Figure 9 summarizes in a flowchart the proposal of clearance of control laws in the Category II PIO perspective. In a real industrial project of control laws, it is necessary to check many requirements in the whole flight envelope. Occurrence of Category II PIO is only one aspect among many others. Moreover, along control laws development some changes might happen, which results new rounds of requirement checks. In this way, a process for clearance of control laws in the Category II PIO perspective, which does not depend on much engineering judgement, has the merit to save time and cover more cases in flight envelope.

OLOP criterion has as strength to indicate potential cases to Category II PIO, so this aspect can be accessed as a first filter in the proposed flowchart. However, the setup of simulation to compare with predictions from OLOP criterion is not trivial (weakness of OLOP criterion). To define a straightforward process, it is proposed a round of simulations in nonlinear model to identify cases with rate saturation that remain for more than 0.5 sec, since the duration of saturation is important, and it is out of OLOP criterion scope. After two steps of filtering (OLOP criterion and cases saturated for more than 0.5 sec), the resultant potential cases are proposed to be checked with pilot-in-the-loop in flight simulator. The delivery of this whole process is a summary indicating which flight conditions are Category II PIO prone.

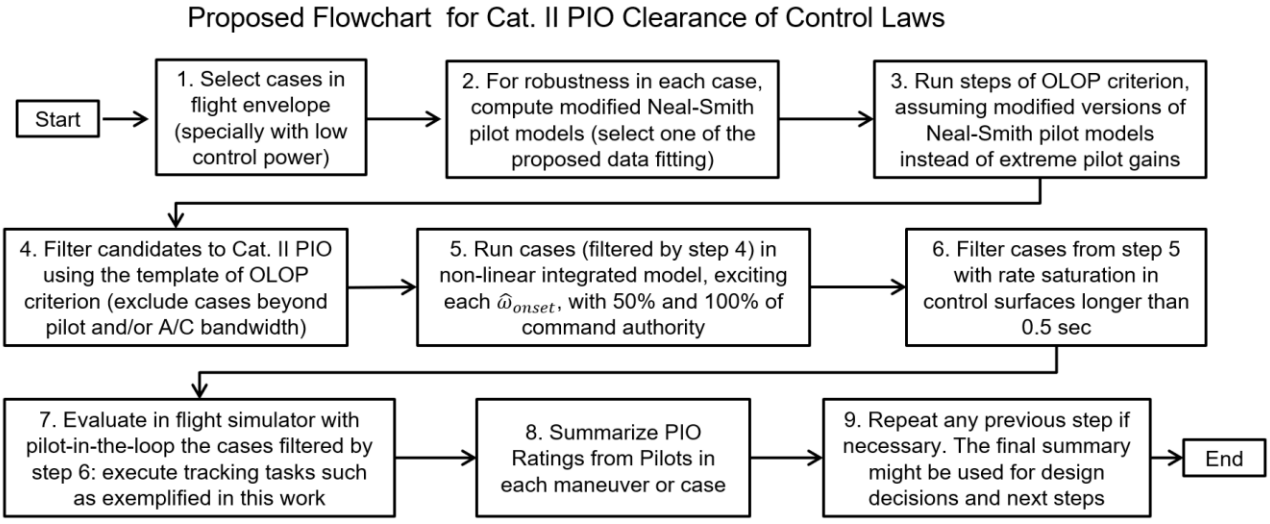

Figure 9 – Proposed Flowchart to predict cases subject to Category II PIO in flight envelope.

Some additional suggestions are listed below to cover the proposed flowchart:

1) Step 1: if it is not possible to cover the whole flight envelope, prioritize at least cases prone to Category I PIO, according to criteria such as Neal and Smith (1971), Gibson (1990), Mitchell and Hoh (1999), Innocenti and Thukral (1991). Other approach is to identify cases with low control power (which traditionally are prone to rate saturation), by computing the maximum roll rate acceleration;

2) Step 2: Modified Neal-Smith pilot models in this work (adapted to lateral-directional axes) was obtained using LOES approach, with definition of a cost function based on errors of magnitudes and phases recorded in flight simulation and replacing exponential by Padé approximation. It is recommended to match pilot models with real pilot data and drive the conclusions around models in this format.

3) Step 3: Adopt modified Neal-Smith model instead of pure pilot gains: example in Figure 8.

4) Step 4: Cases of saturation indicated by OLOP criterion which are not feasible can be ignored (out of scope).

5) Step 5: It is suggested to apply sinusoidal inputs with frequencies ω_{onset} identified in OLOP criterion and different amplitudes (example in Figure 4(a)) in order to achieve ranges of 50% and 100% of command authority.

6) Step 6: Monitor saturation duration and identify cases longer than 0.5 sec. These are the main candidates to PIO.

7) Step 7: Build a test matrix for pilot in simulator including tracking tasks maneuvers (for example Figure 4) in flight conditions filtered by previous steps.

8) Step 8: Organize PIO ratings given by pilots in simulator for each maneuver, in order to map the candidates to Category II PIO in flight envelope.

9) Step 9: If necessary, repeat any preliminary step of flowchart. The conclusion of this whole process is a summary indicating which flight conditions are Category II PIO prone, which might drive future design decisions.

CONCLUSIONS

This work has investigated the OLOP criterion in flight simulator for predictions of Category II PIO (due to rate limiting) and its practical applicability to real industrial designs of control laws for fly-by-wire aircraft. For case study, it was adopted a large transport aircraft and two versions of lateral-directional control laws. Main conclusions are highlighted in the sequence.

In general, the evaluations of pilots in flight simulator confirmed what was predicted by OLOP criterion and it makes sense with the lateral control allocation: "p-Beta" with Method 1 (with spoiler dead zone) is more likely to develop Category II PIO if compared to Method 2 (no spoiler dead zone), since aileron working alone in a period is more exposed to rate saturations.

It is possible to check that higher PIO ratings (worst cases) are associated to cases with longer periods of rate-saturated aileron (more than 0.5 sec). Moreover, some cases with different predictions of Category II PIO according to OLOP criterion have similar PIO ratings given by pilots. It might be justified because rate saturation occurs as predicted by OLOP criterion, but by short periods. Therefore, the pilots did not distinguish significant differences. OLOP criterion gives guidelines to identify Category II PIO prone cases but does not cover the influence of the duration that the control surface remains saturated. It is a significant aggravating to be considered, it is not enough to check only peaks of saturation. Therefore, it was proposed to be considered in the process for clearance of control laws.

The proposed range of pilot pure gains according to original OLOP criterion seems to be excessive. For this work it was possible to match real pilot data (collected from pilot-in-the-loop simulations) with a modified Neal-Smith pilot model (obtained from Lower Order Equivalent System), in order to get a more representative pilot model for offline analysis of OLOP criterion.

Based on previous comments, it is possible to conclude that the original OLOP criterion has some limitations to be applied directly as design tool in real industrial control laws designs. This work raised some limitations and proposed alternatives to overcome in order to define a straight forward process. It is recommended to use the OLOP criterion as a preliminary step to filter cases in the flight envelope (using modified Neal-Smith models instead of pure pilot gains), and additionally to filter again the cases with long periods of rate saturation. The complete process for clearance of control laws, in the Category II PIO perspective, was summarized by a proposed flowchart. In this way, sessions with pilot-in-the-loop have a limited scope, focusing on cases with high probability of rate saturation.

ACKNOWLEDGMENTS

Special thanks to EMBRAER company and ITA (Instituto Tecnológico de Aeronáutica) for providing infra-structure, tools, and personnel (pilots and engineers) which contributed with the development of this work.

REFERENCES

Efremov, A., Efremov, E., and Tiaglik, M., "Advancements in Predictions of Flying Qualities, Pilot-Induced Oscillation Tendencies, and Flight Safety", Journal of Guidance, Control and Dynamics, Vol. 43, No. 1, 2020, pp. 4–14.

USAF. "Military standard - Flying qualities of piloted aircraft", MIL-STD-1797B, 2006.

GARTEUR. "Evaluation of Prominent PIO Susceptibility Criteria", TP-120-01, 1999.

Neal, T. P., and Smith, R. E., "A Flying Qualities Criterion for the Design of Fighter Flight-Control Systems," Journal of Aircraft, Vol. 8, No. 10, 1971.

Gibson, J. C., "Evaluation of alternate handling qualities criteria in highly augmented unstable aircraft," 17th Atmospheric Flight Mechanics Conference, 1990.

Mitchell, D. G., and Hoh, R. H., "Development of methods and devices to predict and prevent pilot-induced oscillations", AFRL-VA-WP-TR-2000-3046, Hoh Aeronautics Inc, USA, 1999.

Innocenti, M., and Thukral, A., "Roll-Performance Criteria for highly Augmented Aircraft," Journal of Guidance, Control and Dynamics, Vol. 14, No. 6, 1991.

Duda, H., "Prediction of Pilot-in-the-Loop Oscillations Due to Rate Saturation", Journal of Guidance, Control and Dynamics, Vol. 20, No. 3, 1997, pp. 581–587.

NASA, "The Simulation of a Jumbo Jet Transport Aircraft Volume II: Modeling Data", NASA D6-30643, USA, 1970.

Gripp, J. A. B., Moreira, M. A. G., Trabasso, L. G., Marinho, C. M. P. "Configuration of aerodynamics model in flight simulator to investigate Pilot-Induced Oscillations and Loss of Control", Proceedings to the XIX International Symposium on Dynamic Problems of Mechanics (DINAME), ABCM, 2023.

Gripp, J. A. B., Moreira, M. A. G., Trabasso, L. G., Marinho, C. M. P. "Control allocation to roll fly-by-wire aircraft with ailerons and roll spoilers", Proceedings to the XIX International Symposium on Dynamic Problems of Mechanics (DINAME), ABCM, 2023.

Gripp, J. A. B., Moreira, M. A. G., Trabasso, L. G., Marinho, C. M. P. "Practical application of Open Loop Onset Point Criterion to predict actuator rate saturation PIO in fly-by-wire aircraft", Proceedings to the XIX International Symposium on Dynamic Problems of Mechanics (DINAME), ABCM, 2023.

Berger, T., Tischler, M. B., Hagerott, S. G., Gangsaas, D., and Saeed, N., "Lateral/directional control law design and handling qualities optimization for a business jet flight control system", AIAA Atm. Flight Mech. Conference, 2013.

Gripp, J. A. B., "Lateral and Directional Control Law Design for Business Jet Employing LQR with Adjust of Transmission Zeros and Gain Scheduling Techniques". Masters of Science (ITA), Brazil, 2015.

Moreira, M. A. G., Gripp, J. A. B., Yoneyama, T., and Marinho, C. M. P., "Longitudinal Flight Control Law Design with Integrated Envelope Protection", Journal of Guidance, Control and Dynamics, 2022, pp. 1–11.

Oliveira, W. R., Matheus, A., Rodamillans, G., Nicola, R. M., Arjoni, D. H., Trabasso, L. G., Villani, E., Silva, E. T.,"Evaluation of the pilot perception in a robotic flight simulator with and without a linear unit," AIAA SciTech Forum, 2019.

Silva, E. T., Penna, S. D., Junior, M. A. O. A., Oliveira, W. R., Villani, E., and Trabasso, L. G., "Flight simulator assisted by a robotic motion platform", AIAA SciTech Forum, 2019.

Mitchell, D. G., and Klyde, D. H., "Recommended Practices for Exposing Pilot-Induced Oscillations or Tendencies in the Development Process", USAF Developmental Test and Evaluation Summit, 2004.

Klyde, D. H., and Mitchell, D. G., Handling Qualities Demonstration Maneuvers for Fixed-Wing Aircraft, Vol. II: Maneuver Catalog, Wright-Patterson AFB, WL-TR-97-3100, 1997.

Klyde, D. H., Schulze, P. C., and Thompson, P. M., "Exposing Unique Pilot Behaviors from Flight Test Data", AIAA Atmospheric Flight Mechanics Conference, 2015.

Berger, T., Tischler, M. B., Hagerott, S. G., Cotting, M. C., Gresham, J. L., George, J. E., Krogh, K. J., d'Argenio, A., and Howland, J. D., "Business Jet Fly-by-Wire Control Laws Handling Qualities Flight Test Assessment," Journal of Guidance, Control and Dynamics, Vol. 44, No. 8, 2021.

McRuer, D. T., "Pilot-Induced Oscillations and Human Dynamic Behavior", NASA4683, NASA, USA, 1995.

Stevens, B., and Lewis, F., "Aircraft control and simulation", John Wiley and Sons, 1992.

Mitchell, D.G. and Hoh, R.H., "Low-Order Approaches to High-Order Systems: Problems and Promises", Journal of Guidance, Control, and Dynamics, Vol. 5, No. 5, 1982.

Morelli, E. A., "Identification of Low Order Equivalent System Models From Flight Test Data", NASA / TM-2000-210117, Langley Research Center, 2000.

RESPONSIBILITY NOTICE

The authors are the only responsible for the printed material included in this paper.